Optically stitched arbitrary fan-sectors with selective polarization states for dynamic manipulation of surface plasmon polaritons

Guo, L. J.; Min, C. J.; Yuan, G. H.; Zhang, C. L.; Wang, J. G.; Shen, Z.; Yuan, X. -C.

2012

Guo, L. J., Min, C. J., Yuan, G. H., Zhang, C. L., Wang, J. G., Shen, Z., et al. (2012). Optically stitched arbitrary fan-sectors with selective polarization states for dynamic manipulation of surface plasmon polaritons. Optics express, 20(22), 24748-24753.

https://hdl.handle.net/10356/101644

https://doi.org/10.1364/OE.20.024748

Optically stitched arbitrary fan-sectors with selective polarization states for dynamic manipulation of surface plasmon polaritons

L. J. Guo,[1] C. J. Min,[1] G. H. Yuan,[2] C. L. Zhang,[1] J. G. Wang,[1] Z. Shen,[1] and X. -C. Yuan[1,*]

[1]*Institute of Modern Optics, Key Laboratory of Optical Information Science & Technology, Ministry of Education of China, Nankai University, Tianjin, 300071, China*

[2]*School of Electrical & Electronic Engineering, Nanyang Technological University, Nanyang Avenue, 639798, Singapore*

[*]*xcyuan@nankai.edu.cn*

Abstract: Novel hybrid-polarized vector beams with radial and azimuthal polarization states in arbitrary fan-sectors are generated and studied for manipulating surface plasmon polaritons (SPPs). The method has high energy conversion efficiency based on an interferometric arrangement with a Dammann vortex phase grating. The polarization states of generated beams are measured by a linear polarizer and show excellent agreement with theoretical predictions. The manipulation properties of the hybrid-polarized beams on SPPs excitation and distribution are demonstrated by both experiments and simulations. The results show that focusing or standing wave patterns of SPPs can be obtained depending on the polarization of the beams.

OCIS codes: (240.6680) Surface plasmons; (260.5430) Polarization.

References and links

1. Q. W. Zhan, "Cylindrical vector beams: from mathematical concepts to applications," Adv. Opt. Photon. **1**(1), 1–57 (2009).
2. L. Novotny, M. R. Beversluis, K. S. Youngworth, and T. G. Brown, "Longitudinal Field Modes Probed by Single Molecules," Phys. Rev. Lett. **86**(23), 5251–5254 (2001).
3. A. Bouhelier, M. Beversluis, A. Hartschuh, and L. Novotny, "Near-Field Second-Harmonic Generation Induced by Local Field Enhancement," Phys. Rev. Lett. **90**(1), 013903 (2003).
4. N. Hayazawa, Y. Saito, and S. Kawata, "Detection and characterization of longitudinal field for tip-enhanced Raman spectroscopy," Appl. Phys. Lett. **85**(25), 6239–6241 (2004).
5. B. H. Jia, X. S. Gan, and M. Gu, "Direct measurement of a radially polarized focused evanescent field facilitated by a single LCD," Opt. Express **13**(18), 6821–6827 (2005).
6. H. Kano, S. Mizuguchi, and S. Kawata, "Excitation of surface plasmon polaritons by a focused laser beam," J. Opt. Soc. Am. B **15**(4), 1381–1386 (1998).
7. K. J. Moh, X.-C. Yuan, J. Bu, S. W. Zhu, and B. Z. Gao, "Surface plasmon resonance imaging of cell-substrate contacts with radially polarized beams," Opt. Express **16**(25), 20734–20741 (2008).
8. R. Zia, J. A. Schuller, A. Chandran, and M. L. Brongersma, "Plasmonics: the next chip-scale technology," Mater. Today **9**(7-8), 20–27 (2006).
9. K. J. Moh, X.-C. Yuan, J. Bu, S. W. Zhu, and B. Z. Gao, "Radial polarization induced surface plasmon virtual probe for two-photon fluorescence microscopy," Opt. Lett. **34**(7), 971–973 (2009).
10. X. L. Wang, J. P. Ding, W. J. Ni, C. S. Guo, and H. T. Wang, "Generation of arbitrary vector beams with a spatial light modulator and a common path interferometric arrangement," Opt. Lett. **32**(24), 3549–3551 (2007).
11. X. M. Gao, J. Wang, H. T. Gu, and W. D. Xu, "Focusing properties of concentric piecewise cylindrical vector beam," Optik (Stuttg.) **118**(6), 257–265 (2007).
12. G. Machavariani, Y. Lumer, I. Moshe, A. Meir, and S. Jackel, "Spatially-variable retardation plate for efficient generation of radially- and azimuthally-polarized beams," Opt. Commun. **281**(4), 732–738 (2008).
13. U. Levy, C. H. Tsai, L. Pang, and Y. Fainman, "Engineering space-variant inhomogeneous media for polarization control," Opt. Lett. **29**(15), 1718–1720 (2004).
14. M. Stalder and M. Schadt, "Linearly polarized light with axial symmetry generated by liquid-crystal polarization converters," Opt. Lett. **21**(23), 1948–1950 (1996).

#174857 - $15.00 USD Received 23 Aug 2012; revised 28 Sep 2012; accepted 7 Oct 2012; published 15 Oct 2012

15. K. J. Moh, X.-C. Yuan, J. Bu, R. E. Burge, and B. Z. Gao, "Generating radial or azimuthal polarization by axial sampling of circularly polarized vortex beams," Appl. Opt. **46**(30), 7544–7551 (2007).
16. E. Ozbay, "Plasmonics: merging photonics and electronics at nanoscale dimensions," Science **311**(5758), 189–193 (2006).
17. W. L. Barnes, A. Dereux, and T. W. Ebbesen, "Surface plasmon subwavelength optics," Nature **424**(6950), 824–830 (2003).
18. L. L. Yin, V. K. Vlasko-Vlasov, J. Pearson, J. M. Hiller, J. Hua, U. Welp, D. E. Brown, and C. W. Kimball, "Subwavelength focusing and guiding of surface plasmons," Nano Lett. **5**(7), 1399–1402 (2005).
19. A. Imre, V. K. Vlasko-Vlasov, J. Pearson, J. M. Hiller, and U. Welp, "Multiplexing surface plasmon polaritons on nanowires," Appl. Phys. Lett. **91**(8), 083115 (2007).
20. C. H. Zhou and L. R. Liu, "Numerical study of Dammann array illuminators," Appl. Opt. **34**(26), 5961–5969 (1995).
21. I. Moreno, J. A. Davis, D. M. Cottrell, N. Zhang, and X.-C. Yuan, "Encoding generalized phase functions on Dammann gratings," Opt. Lett. **35**(10), 1536–1538 (2010).
22. R. Wang, C. L. Zhang, Y. Yang, S. Z. Zhu, and X.-C. Yuan, "Focused cylindrical vector beam assisted microscopic pSPR biosensor with an ultra wide dynamic range," Opt. Lett. **37**(11), 2091–2093 (2012).

1. Introduction

In recent years, vector beams have attracted increasing attention due to their interesting polarization properties [1], especially when the cylindrical symmetric radially polarized (RP) beams are found in many applications including particle acceleration, fluorescent imaging, second-harmonic generation, Raman spectroscopy, and surface plasmon polaritons (SPPs) sensing and imaging [2–9]. It is noted that SPPs can be excited by a focused vector beam when the incident angle and polarization state are required to meet the SPPs excitation condition, namely the surface plasmon resonance (SPR) angle and transverse magnetic (TM) polarization. In this connection, a novel vector beam design with artificially tailored incident angle and localized polarization manipulation could give rise to the diverse SPP applications in the microscopic configuration. Recently, vector beams with different polarization states in annular zones have been reported [10], which can be applied to manipulation of beam focusing and optical trapping [11]. However, such annularly distributed hybrid-polarized beams cannot be used for manipulation of SPPs when focused on a metal film, due to the fact that the annular zone corresponding to the SPR angle always has the same polarization state. Thus, in order to manipulate SPPs, vector beams with radial and azimuthal polarization states distributed in fan-sectors are proposed accordingly.

In this paper, we investigate the generation of a novel hybrid-polarized vector beam with optically stitched radial and azimuthal polarization states in arbitrary fan-sectors, and consider its manipulation property on SPPs excitation and distribution. Our method uses an interferometric arrangement in combination with a simple phase plate and a Dammann vortex phase grating, which shows higher energy conversion efficiency than the interferometric arrangement with a spatial light modulator (SLM) [10], and easier implementation than the method of direct polarization conversion scheme [12–15]. The polarization states of resultant beams measured by a linear polarizer show excellent agreement with theoretical predictions. The excitation of SPPs modulated by different distributions of radial and azimuthal polarization states are experimentally verified by the discrete dark lines at the back focal plane of a high NA total internal reflection fluorescence (TIRF) lens. The excited SPPs intensity distribution is also investigated by finite difference time domain (FDTD) simulations and vectorial diffraction theory, which clearly show that the SPPs intensity distribution is strongly influenced by the polarization distribution of the beam. It is worth to note that, compared to the methods for excitation and modulation of SPPs by various metallic nanostructures [16–19], our method of using optically stitched hybrid-polarized vector beams benefits from the structureless excitation of SPPs with a dynamic configuration, therefore reducing the requirements for fabrication of complex structures on the nanometer scale.

The remainder of the paper is organized as follows. In Section 2, we introduce the generation method of the hybrid-polarized vector beam, and verify the polarization states of generated beams by a linear polarizer. The manipulation properties of generated beams on SPPs

#174857 - $15.00 USD Received 23 Aug 2012; revised 28 Sep 2012; accepted 7 Oct 2012; published 15 Oct 2012

excitation and distribution are presented in Section 3. Finally, our conclusions are summarized in Section 4.

2. Generation of the fan-sector distributed hybrid-polarized vector beams

Since cylindrical vector beams obey cylindrical symmetry both in amplitude and polarization, each point of a generalized cylindrical vector beam has a polarization rotated by φ from its radial direction, which can be written as a Jones vector $\mathbf{E}_{\mathrm{CVB}}$ and decomposed as

$$\mathbf{E}_{\mathrm{CVB}} = \begin{pmatrix} \cos(\varphi+\phi) \\ \sin(\varphi+\phi) \end{pmatrix} = \frac{1}{2} e^{i(\varphi+\phi)} \begin{pmatrix} 1 \\ -i \end{pmatrix} + \frac{1}{2} e^{-i(\varphi+\phi)} \begin{pmatrix} 1 \\ i \end{pmatrix} = \frac{1}{2} e^{i\varphi} e^{i\phi} \begin{pmatrix} 1 \\ -i \end{pmatrix} + \frac{1}{2} e^{-i\varphi} e^{i(2\pi-\phi)} \begin{pmatrix} 1 \\ i \end{pmatrix} \quad (1)$$

where φ is the azimuthal angle. The results show that a generalized cylindrical vector beam is the superposition of a positive vortex phase encoded right-handed circularly polarized beam and a negative vortex phase encoded left-handed circularly polarized beam, and different kinds of cylindrical vector beams can be generated by changing the phase difference (2π-2φ) between the two constituent beams. Based on this principle, vector beams with various polarization states in different sectors can be optically stitched accordingly by adjusting such a phase difference for different sectors. If we consider that the cross section of a laser beam is divided into n sectors (n = 1, 2, 3,…), and each sector has different polarization state described by φ_i (i = 1, 2, 3,…, n), then a hybrid-polarized vector beam can be generated by inserting a phase plate embedded with the phase of (2π-$2\varphi_i$) for each sector in one path of an interferometric arrangement.

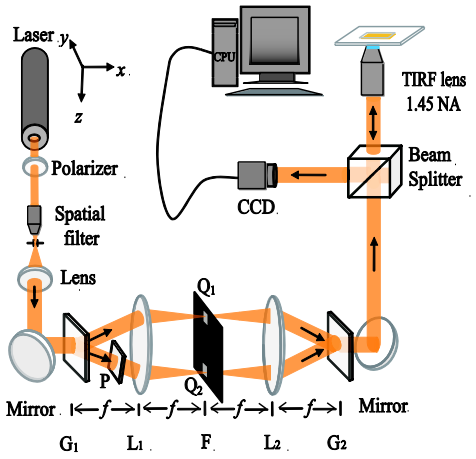

Fig. 1. Schematic of the experimental setup. G_1, Dammann vortex phase grating; P, phase plate; L_1, lens; Q_1, quarter wave-plate; Q_2, quarter wave-plate; F, Fourier plane; L_2, lens; G_2, Dammann phase grating. The gap between the objective lens and the glass substrate is filled with index matching oil.

The experimental setup is shown in Fig. 1. A He-Ne laser beams (λ = 632.8 nm) polarized along the x axis passes through a spatial pinhole filter and a lens, then illuminates on a Dammann vortex phase grating (G_1). G_1 is the superposition of a Dammann binary phase grating and a vortex phase with the charge of + 1 where the Dammann binary phase grating has equal widths for phase shifts of 0 and π rad in a period. The special structure of G_1 making it split the ± 1st diffracted orders with equal intensity and has ~81% diffraction efficiency for the ± 1st orders [20, 21], which is much larger than the hologram reconstructed either by an SLM [10] or amplitude-modulated diffractive elements. A phase plate (P) divided into n sectors (n = 1, 2, 3,…) and embedded with the phase of 2π-$2\varphi_i$ (i = 1, 2, 3,…, n) is used in one path of the ± 1st orders for polarization modulation. Then the ± 1st orders are chosen to pass through a spatial

#174857 - $15.00 USD Received 23 Aug 2012; revised 28 Sep 2012; accepted 7 Oct 2012; published 15 Oct 2012

filter (F) with two separate open apertures placed at the Fourier plane in a 4-*f* system. Two $\lambda/4$ wave-plates (Q_1 and Q_2) located at the open apertures are used to generate a pair of orthogonal right-handed and left-handed circularly polarized beams. After the 4-*f* system, the ± 1st orders are recombined to generate the expected hybrid-polarized vector beam by a Dammann binary phase grating (G_2) whose period matches G_1 with a combination efficiency of ~39% for the ± 1st orders. The generated beam is finally focused by a TIRF (Olympus Plan APO 100 × /NA 1.45) objective lens to excite SPPs on a gold film (thickness of 45 nm) and recorded by a CCD camera. The incident beam through the objective lens provides a wide range of angle (0-71.8°) including the SPR angle (~44.2°).

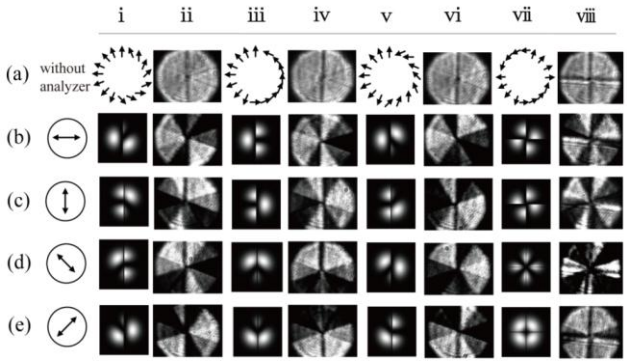

Fig. 2. Theoretical and experimental results of the far-field intensity distribution without and with linear polarizer for four kinds of hybrid vector beams.

To obtain the vector beams with different polarization distribution, here we fabricate four phase plates by using a mask aligner (Suss MJB4). A laser direct writer (Heidelberg/DWL66) is employed to fabricate two different masks, and two kinds of photoresists are used to fabricate these phase plates, which are AR-N 4340 and RZJ 304. Three of them are divided into two equal sectors (semi-circles): one sector is embedded with the phase of 0, the other sector is embedded with the phase of $3\pi/2$, π, and $\pi/2$ respectively. The fourth phase plate is divided into four equal sectors, with the second and fourth sectors embedded with the phase of π and the others with the phase of 0. The first sector starts from the positive x axis, and increases in an anticlockwise direction. The generated beam is observed in free space, and the intensity distribution of the beam after encountering a linear polarizer is recorded by a CCD camera. The far-field intensity distributions of the four kinds of hybrid vector beams obtained from CCD are shown in Fig. 2. The polarization distributions of the first three hybrid vector beams with different polarization states in two sectors (n = 2) are schematically shown in Fig. 2(i-a), Fig. 2(iii-a), and Fig. 2(v-a), where the left sector has the mode of 0 (pure radial polarization) and the right sector has the mode of $\pi/4$, $\pi/2$, $3\pi/4$ respectively. Figure 2(vii-a) shows the polarization distribution of a hybrid vector beam with n = 4 and $\varphi_1 = \varphi_3 = 0$ (pure radial polarization), $\varphi_2 = \varphi_4 = \pi/2$ (pure azimuthal polarization). The numerically simulated intensity distributions after a linear polarizer with orientation of (b) horizontal, (c) vertical, (d) 135°, and (e) 45°with respect to the + x axis are also shown in columns i, iii, v, and vii respectively. In comparison, the experimental results for the four kinds of hybrid vector beams are shown in columns ii, iv, vi, and viii respectively. It is obvious that the experimental results agree well with the theoretical predictions, proving the successful generation of the expected hybrid-polarized vector beams by our method. The dark lines observed in the intensity distribution are due to the phase jump in the phase plate. The central dark spot originates from the polarization singularity in the beam center. Compared to the pure radially or azimuthally polarized beam where only two spots are expected after a linear polarizer, here our generated hybrid-polarized vector beams show various intensity patterns due to the non-cylindrical symmetry distribution of the electric vector in the beam cross section.

#174857 - $15.00 USD Received 23 Aug 2012; revised 28 Sep 2012; accepted 7 Oct 2012; published 15 Oct 2012

3. Manipulation of SPPs using the fan-sector distributed hybrid-polarized vector beams

When the hybrid-polarized vector beams generated in above section are strongly focused onto a metal-dielectric interface, only the radially-polarized sectors have TM polarization with respect to the metal-dielectric interface, while the azimuthally-polarized (AP) sectors are TE polarized, so SPPs can only be excited within the sectors of radial polarization, which can be employed to manipulate the excitation and distribution of SPPs.

We firstly study the property of the SPPs excitation by the hybrid-polarized beams. As shown in the experiment setup (Fig. 1), the hybrid-polarized beam focused by a TIRF objective lens completely fills the back aperture of the lens, and thus provides a wide range of angles including the SPR angle as mentioned above. At the SPR angle, the light from the incident laser beam is effectively coupled to the SPPs mode at the gold-air interface, resulting a near-zero reflection. Thus, the intensity recorded by CCD at the back focal plane of the objective lens corresponding to SPR angle decreases sharply and shows a clear dark region.

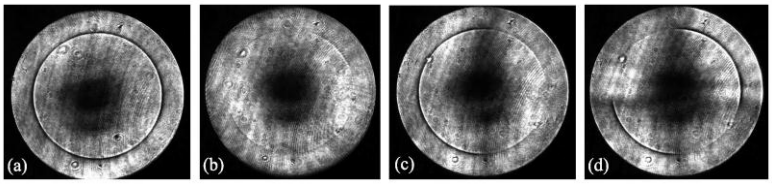

Fig. 3. Experimental results of intensity distributions at the back focal plane of the objective lens for (a) RP beam, (b) AP beam, (c) hybrid-polarized beam with n = 2 (left sector is RP, right sector is AP), and(d) hybrid-polarized beam with n = 4 (the 1st and 3rd quadrants are RP, the 2nd and 4th quadrants are AP) illumination.

Intensity distributions at the back focal plane of the objective lens for four different modes of beams are shown in Fig. 3. Because of the cylindrical symmetry of RP beam, a dark ring is observed in Fig. 3(a), which indicates that SPPs are excited in all directions. The angle corresponding to the dark ring is calculated to be 44.9° from the CCD image, which is in good agreement with the theoretical SPR angle (~44.2°). In contrast, since AP beam is totally reflected by the gold film without SPPs excitation, there is no obvious dark region shown in Fig. 3(b). In Fig. 3(c), a dark semi-ring in the left side is observed, because the hybrid-polarized beam with n = 2 only excite SPPs in the left sector of radial polarization. In Fig. 3(d), the hybrid-polarized beam with n = 4 excites SPPs in the 1st and 3rd quadrant sectors of radial polarization, therefore two dark arc-lines appear along these two directions. Note that the unobvious dark arc-line appear in Fig. 3(b) can be attributed to the system error coming from the imperfect control of phase difference between the optical path lengths in the two arms.

We also study the intensity distributions of SPPs on gold film depending on the polarization distribution of the hybrid-polarized beams, shown in Fig. 4. We employ a commercial three-dimensional FDTD software (Rsoft 8.01) to simulate the SPPs intensity distribution. The dielectric constant of gold is $\varepsilon_m = -9.7997 + 1.9649i$ at 632.8 nm wavelength, and all results are normalized. In the case of a single sector excitation, as shown in Figs. 4(a) and 4(b), the excited SPPs propagate toward the center and form a bright spot with asymmetry intensity distribution because of the constructive interference of SPPs, then propagate away from the center. The propagation length of SPPs at a 45nm gold/air interface is around 28 μm, and the reason why it seems to be shorter in Figs. 4(a) and 4(b) than the expected value is that the remarkably enhanced central focal spot increases the image contrast and thus it becomes difficult to distinguish the divergingly propagating SPPs after the focus. The shape and size of the spot are strongly dependent on the arc-length of the radially-polarized sectors. Figure 4(c) shows the SPPs intensity distribution for hybrid-polarized beam with n = 4 (radial polarization in 1st and 3rd quadrants). As expected, two groups of counter-propagating SPPs interfere with each other and form SPPs standing waves with a field-enhanced central lobe and two side-lobes on the

#174857 - $15.00 USD Received 23 Aug 2012; revised 28 Sep 2012; accepted 7 Oct 2012; published 15 Oct 2012

metal film. The period of the standing waves is evaluated to be 299 nm. Figure 4(d) shows the SPPs intensity distribution for hybrid-polarized beam with n = 8 (radial polarization in 4 sectors), a central spot with enhanced localized field and four side-lobes are yielded, similar to the SPPs virtual probe [9]. The FWHM of the main lobe is 224 nm and beyond the diffraction limit. The SPPs intensity distributions for the four kinds of hybrid-polarized vector beams are also simulated using the vectorial diffraction theory [1] as shown in Figs. 4(e)-4(h), the results are in good agreement with the FDTD calculations. The simulated results demonstrate that the SPPs intensity pattern can be effectively modulated by changing the polarization distribution of the hybrid-polarized beam.

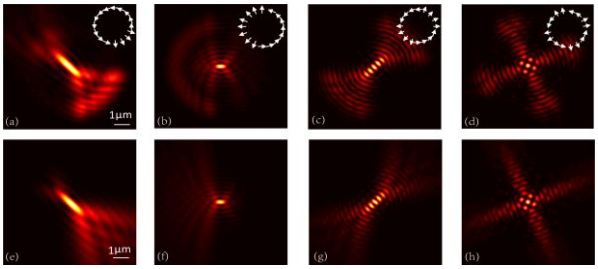

Fig. 4. FDTD simulated results of normalized SPPs intensity distributions for hybrid-polarized beam with radial polarization (a) only in a quadrant sector, (b) in left semi-circle, (c) in 1st and 3rd quadrants, (d) in 4 sectors of 0~45°, 90~135°, 180~225°, 270~315°. (e)-(h) are the corresponding numerically simulated results using vectorial diffraction theory. All inserts indicate the polarization distribution of the hybrid-polarized beams.

The manipulation properties of hybrid-polarized beams on SPPs excitation and distribution have great potential in many applications, such as plasmonic communication and bio-sensing. For instance, the results shown in Fig. 4(a) and 4(b) can be applied to subwavelength focusing and guiding of plasmonic signals [18] without complex metallic nanostructures. The hybrid-polarized beams with equal intensity of RP and AP parts have application in microscope differential-interferential phase-type SPR biosensor [22] to make the RP and AP beams travel through the same optical path, and therefore reducing the system error and further enhancing the sensitivity.

4. Conclusions

In conclusion, optically stitched hybrid-polarized vector beams with radial and azimuthal polarization states in different fan-sectors are generated and studied for manipulating SPPs excitation and distribution. The proposed method, comprising of an interferometric arrangement with a simple phase plate and a Dammann vortex phase grating, shows higher energy conversion efficiency. The polarization states of generated beams are measured by a linear polarizer and show excellent agreement with theoretical predictions. The manipulation properties of generated hybrid-polarized beams on SPPs excitation and distribution are demonstrated by both experiments and simulations. It is clearly shown that the focusing and standing wave patterns of SPPs are strongly depending on the polarization distribution of the hybrid-polarized beams. Finally, we note that such hybrid-polarized beams have great potential applications in plasmonic communication and bio-sensing.

Acknowledgments

This work was partially supported by the National Natural Science Foundation of China under grant no. (10974101, 61036013, 61138003) and the Ministry of Science and Technology of China under grant No. 2009DFA52300 for China-Singapore collaborations. XCY acknowledges the support given by Tianjin Municipal Science and Technology Commission under grant no. 11JCZDJC15200.

#174857 - $15.00 USD Received 23 Aug 2012; revised 28 Sep 2012; accepted 7 Oct 2012; published 15 Oct 2012